Origin of polar organic sulfur compounds in immature crude oils revealed by ESI FT-ICR MS

Weimin Liu [a,b], Yuhong Liao [a,*], Quan Shi [c], Chang Samuel Hsu [c,d,e], Bin Jiang [a], Ping'an Peng [a]

[a] State Key Laboratory of Organic Geochemistry, Guangzhou Institute of Geochemistry, Chinese Academy of Sciences, Wushan, Guangzhou 510640, PR China
[b] University of Chinese Academy of Sciences, Yuquan Road, Beijing 100049, PR China
[c] State Key Laboratory of Heavy Oil Processing, China University of Petroleum, Beijing 102249, PR China
[d] Petro Oil Consulting, Tallahassee, FL 32312, USA
[e] Department of Chemical and Biomedical Engineering, Florida A&M University/Florida State University, Tallahassee, FL 32310, USA

ARTICLE INFO

ABSTRACT

Organic sulfur compounds (OSCs) are abundant in immature crude oils, including "polar" OSCs that are defined here as compounds containing one or more heteroatom(s) in addition to sulfur atoms having sufficient polarity to be analyzable by electrospray ionization (ESI) without derivatization. An understanding of the origins of polar OSCs in crude oils has been hampered by limitations in their analytical characterization. In this paper, we employed a high field (9.4 T) Fourier transform ion cyclotron resonance mass spectrometry (FT-ICR MS) coupled with ESI to study the sulfur-rich immature crude oils from the Jianghan Basin in China. The results show that the polar OSCs usually have non-sulfur counterparts, i.e., heteroatom-containing compounds without sulfur, with similar carbon number ranges, but slightly lower DBE (double bond equivalence) distributions. The similar or even identical carbon number distributions of the polar OSCs and their non-sulfur counterparts indicate their inheritance from the same precursors. The sulfur rings in polar OSCs are formed by intramolecular sulfurization that leads to the increases in DBEs compared to their non-sulfur counterparts. The results also indicate that the number of sulfur rings that can be formed in polar OSCs is largely controlled by the number of available reactive functional groups in their precursors. This paper extends our knowledge of intramolecular sulfurization during early diagenesis, especially for polar heteroatom-containing compounds.

1. Introduction

Organic sulfur compounds (OSCs) in immature sediments and crude oils have a structural resemblance with some geologically occurring hydrocarbons (Valisolalao et al., 1984; Sinninghe Damsté et al., 1988, 1989a, 1989c, 1989d, 1990; Kohnen et al., 1990a, 1990b; Eglinton et al., 1994; Werne et al., 2000) and carbohydrates (Sinninghe Damsté et al., 1989b; Kok et al., 2000; van Dongen et al., 2003). Most of the sulfur in these OSCs is believed to be introduced by the incorporation of inorganic sulfides (H_2S, HS_x^-, and S_x^-) into functionalized hydrocarbons and carbohydrates during early diagenesis under favorable conditions (anoxic with low amounts of available ferric ions) (Sinninghe Damsté et al., 1988, 1989a, 1989b; Kohnen et al., 1990a; Eglinton et al., 1994; Werne et al., 2003). The sulfur incorporation (sulfurization) is usually abiotic and relies on the presence of reactive functional groups such as carbon-carbon double bonds in hydrocarbons and carbohydrates (de Graaf et al., 1992; Schouten et al., 1994). Hydrocarbons that lack reactive functional groups are preserved in sediments without being sulfurized (Sinninghe Damsté et al., 1988, 1989a; Wakeham et al., 1995).

The reaction of inorganic sulfides with the functional groups of hydrocarbons and carbohydrates involves several chemical reactions. For example, a nucleophilic addition that follows the Markovnikov rule often takes place with compounds possessing carbon-carbon double bonds, and a nucleophilic substitution generally occurs to the oxo-group of ketones and aldehydes (de Graaf et al., 1992; Schouten et al., 1994). The reaction of organic molecules with inorganic sulfides can be differentiated as 'intramolecular' and 'intermolecular' sulfurization that yield OSCs with very different structural characteristics (Sinninghe Damsté et al., 1988, 1989a, 1989b). Intramolecular sulfurization often produces low molecular weight OSCs that contain saturated sulfur rings (e.g., thiolane or thiane structure) (Sinninghe Damsté et al., 1989c; Werne et al., 2000). The formation of each saturated sulfur

---

* Corresponding author.
 E-mail address: liaoyh@gig.ac.cn (Y. Liao).

ring leads to an increase in double bond equivalents (DBEs) by 1. The saturated sulfur ring can be further aromatized to thiophenes, resulting in an additional increase in DBEs by 2, or 3 from the original precursor, during thermal maturation (Sinninghe Damsté et al., 1989b, 1998a; Kohnen et al., 1990a). These intramolecular sulfurization products usually retain the original carbon skeletons of their precursor hydrocarbons or carbohydrates (de Graaf et al., 1992; Schouten et al., 1994). Intermolecular sulfurization usually produces macromolecules with acyclic sulfur functional groups, such as thiols and thioethers, with no increases in DBEs (Sinninghe Damsté et al., 1988, 1989a; Tegelaar et al., 1989; Eglinton et al., 1994; Kok et al., 2000; Liu et al., 2010a, 2010b).

Previous studies of OSCs identified in immature oils analyzed GC-amenable compounds or decomposed species generated via flash pyrolysis or chemical degradation (Kohnen et al., 1989, 1993; Sinninghe Damsté and de Leeuw, 1990). These compounds usually do not contain heteroatoms other than sulfur. Even those studies on sulfurization of carbohydrates were mostly concerned about the substitution of their oxo-group by inorganic sulfides (Sinninghe Damsté et al., 1998b; van Dongen et al., 2003). A large portion of OSCs are not sufficiently volatile or thermally stable to be analyzed by GC.

In recent decades, the development of Fourier-transform ion cyclotron resonance mass spectrometry (FT-ICR MS) has shed light on the comprehensive analyses of complex organic mixtures (Hsu et al., 1994, 2011). Coupled with electrospray ionization (ESI), FT-ICR MS can selectively detect a wide range of polar heteroatom-containing compounds in organic mixtures with high mass resolution and mass accuracy (Kujawinski, 2002; Hughey et al., 2002b; Bae et al., 2010; Li et al., 2010; Shi et al., 2010c; Chen et al., 2012; Liao et al., 2012; Colati et al., 2013; Pan et al., 2013, 2017; Cho et al., 2014). Polar OSCs that contain one or more heteroatoms in addition to sulfur have been reported in many immature oils (Liu et al., 2010a; Lu et al., 2014; Oldenburg et al., 2017). However, the origin of these OSCs remains largely unanswered.

In this paper, a high-field (9.4 T) FT-ICR MS coupled with ESI was employed to study the polar OSCs in two immature sulfur-rich crude oils from the Jianghan Basin in China. The distributions of polar OSCs were compared with those of corresponding non-sulfur heteroatom-containing compounds in the crude oils. We hypothesize that the similarity in their distributions provides evidence for precursor species for the OSCs.

2. Samples and experimental methods

2.1. Samples

Two immature sulfur-rich crude oils, JH-1 and JH-2, were collected from the Jianghan Basin, China. They differ considerably in bulk composition. The sulfur content in the JH-1 and JH-2 oil are 6.43 wt% and 1.89 wt%, respectively. Saturated hydrocarbon accounted for 14.4 wt% and 51.0 wt%, respectively of the C_{15+} fraction of the JH-1 and JH-2 oils.

2.2. GC–MS analysis

Each crude oil was separated into maltene and asphaltene fractions using a deasphaltening procedure described in Liao et al. (2009). The maltene fraction was subsequently fractionated into saturated, aromatic and resin fractions by silica gel/alumina column chromatography eluting with n-hexane, DCM/n-hexane (3:1, v:v), and DCM/methanol (2:1, v:v), respectively. The saturated fraction was analyzed by GC–MS.

GC–MS analyses were performed using a Thermo Scientific Trace GC Ultra gas chromatography coupled with a Thermo

Scientific Trace DSQ II mass spectrometer. An HP-1 fused silica capillary column (30 m × 0.25 mm i.d. × 0.25 μm film thickness) was used for separation. The column was held at 40 °C for 2 min and then ramped to 290 °C at a rate of 4 °C/min with a final temperature holding time of 20 min. Helium was used as a carrier gas at a constant flow rate of 1.2 mL/min. The ion source was maintained at 260 °C and operated in the electron-impact ionization (EI) mode with electron beam energy of 70 eV. The mass range was set at m/z 50–650, with a scanning cycle at 100 ms.

2.3. ESI FT-ICR MS analyses

Each oil sample was dissolved in toluene to produce a 10 mg/mL solution. A total of 20 μL sample solution was further diluted with 1 mL of toluene/methanol (1:3, v:v) mixture. $HCOONH_4$ (15 μL) and NH_4OH (15 μL) were added to the sample solution to enhance the ionization efficiency under positive- and negative-ion ESI modes, respectively (Lu et al., 2016; Pan et al., 2017).

The MS analysis was performed on a SolariX XR FT-ICR MS (Bruker Daltonik GmbH, Bremen, Germany) equipped with a 9.4 T refrigerated actively shielded superconducting magnet (Bruker Biospin, Wissembourg, France) and Paracell analyzer cell located at the Guangzhou Institute of Geochemistry, Chinese Academy of Sciences. The sample solution was injected into the electrospray source using a syringe pump at a constant rate of 180 μL/h. Under positive-ion ESI mode, the conditions were −4.0 kV spray shield voltage, −4.5 kV capillary column introduced voltage, and 240 V capillary column end voltage. Under negative-ion ESI mode, the conditions were 4.0 kV spray shield voltage, 4.5 kV capillary column introduced voltage, and 240 V capillary column end voltage. The ions were stored in an argon-filled collision cell for 1 s and then transferred to the ICR cell with a 0.7 ms time-of-flight window. A total of 128 scans were accumulated and averaged to improve the signal-to-noise ratio of the mass spectrum. The mass range was 200–800 Da. The size of the dataset was 4 M words.

The mass spectrum was calibrated using alkyl pyridines and fatty acids in high abundances under positive- and negative-ion ESI modes, respectively. Peaks with relative abundances greater than 6 times the standard deviation of the baseline noise level were exported to a spreadsheet. Data analysis was performed using custom software described in detail in Shi et al. (2010b, 2013).

3. Results

3.1. The composition of saturated fractions revealed by GC–MS

The distribution of saturated hydrocarbons of the immature JH-1 and JH-2 oils are revealed by total ion chromatograms (TICs) (Fig. 1). The n-alkanes extend to C_{34}, with n-C_{24} being the most abundant in both crude oils. The n-alkanes exhibit an even-over-odd preference in the carbon number range of C_{18} to C_{30}. The odd-even-preference (OEP) values of n-alkanes in JH-1 and JH-2 are 0.76 and 0.86, respectively. Phytane is the most abundant saturated hydrocarbon and the pristane/phytane ratios of JH-1 and JH-2 are 0.15 and 0.30, respectively.

3.2. The composition of heteroatomic compounds revealed by ESI FT-ICR MS

The broadband positive- and negative-ion ESI FT–ICR mass spectra of crude oils are provided in Supplementary Fig. S1. Some pronounced peaks in the negative-ion spectra of crude oils, such as $C_{16}H_{32}O_2$, $C_{18}H_{36}O_2$, and $C_{17}H_{26}O_4$, are contaminants in the system (Pan et al., 2017), and are excluded in the data analysis
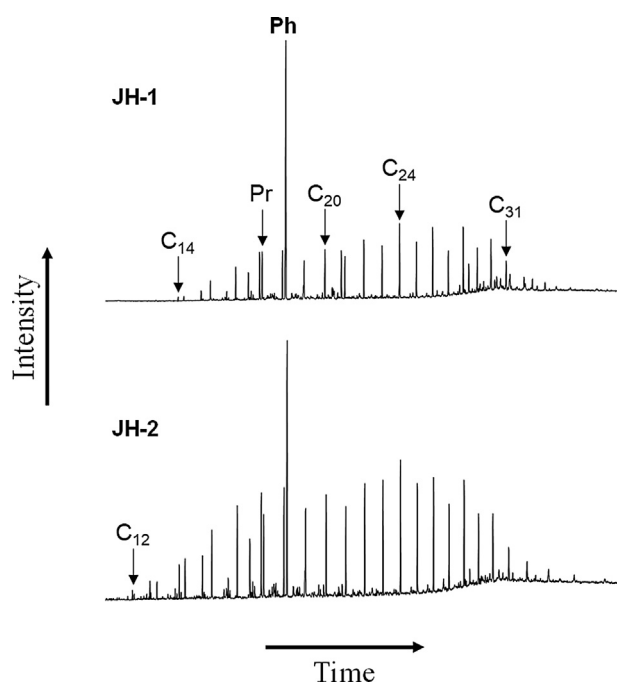
Fig. 1. Total ion chromatograms of the JH-1 and JH-2 saturate fractions.

discussed below. To simplify the dataset obtained from FT-ICR MS analysis, molecular ion peaks that can be assigned with a formula were sorted into different heteroatomic classes (N, O, S) and compound types in double bond equivalence (DBE) and carbon number. Several heteroatomic classes were identified in the oils, including S_x, N_1, and N_1S_x classes under positive-ion ESI mode and N_1, N_1S_x, O_x, and O_xS_y classes under negative-ion ESI mode. Fig. 2 shows the major heteroatomic classes in the spectra. The OSCs assigned in JH-1 are more abundant than those in JH-2, which is consistent with the total sulfur contents of these oils.

Weakly polar sulfur-containing compounds are in general not ionizable by ESI without derivatization (Andersson, 2017; Han et al., 2018). In our studies, we found the incorporation with other non-sulfur heteroatom-containing compounds as substructures

into more "polar" species enabled the ionization of sulfur-containing compounds under ESI conditions without derivatization. Hence we classified these compounds as "polar" OSCs. Relative ion abundance plots, i.e., DBE vs carbon number, from negative- and positive-ion ESI analyses, illustrate the distribution of N_1S_{0-2} (Figs. 3 and 4), O_1S_{0-2} (Figs. 5 and 6), and S_{1-5} (Fig. 7) species.

3.3. N_1 and N_1S_x species detected by negative-ion ESI

N_1 species detected under negative-ion ESI mode were assigned to neutral nitrogen compounds having a pyrrolic structure (i.e., a nitrogen atom in a five-member ring) (Bae et al., 2010; Liao et al., 2012; Pan et al., 2013; Shi et al., 2013). In the JH-1 and JH-2 oils, the detected carbon number of N_1 species ranges from 14 to 43 and 14 to 48, the DBEs range from 6 to 17 and 9 to 20, and the minimum DBEs are 6 and 9, respectively (Fig. 3A and B). The N_1 species exhibit a bimodal distribution of DBEs in both oils. The most abundant N_1 species have DBEs of 6 and 9 in JH-1 and DBEs of 9 and 12 in JH-2. N_1 species with DBEs of 6, 9, and 12 correspond to alkyl indoles, carbazoles, and benzocarbazoles, respectively (Shi et al., 2010d; Liao et al., 2012; Pan et al., 2013; dos Santos Rocha et al., 2018).

The N_1S_x species were assigned to pyrrolic substructures, as compounds containing only sulfur generally cannot be ionized by negative-ion ESI (Liu et al., 2010a, 2010b; Shi et al., 2010a; Lu et al., 2014). N_1S_1 species in JH-1 and JH-2 oils range in carbon numbers from 16 to 39 and 16 to 44, in DBEs from 7 to 18 and 10 to 19 with minimum DBEs of 7 and 10 (Fig. 3C and D). These are one higher than seen for the N_1 species. By analogy, the N_1S_1 species with a DBE of 7 in JH-1 could contain an indole substructure with a saturated sulfur ring, while those with a DBE of 10 in JH-2 could contain a carbazole substructure with a saturated sulfur ring. These sulfur-containing neutral nitrogen compounds also show bimodal DBE distributions as neutral nitrogen compounds. The abundant N_1S_1 species have DBEs of 8 and 11 in JH-1 and DBEs of 11 and 14 in JH-2. The N_1S_1 species with a DBE of 8, 11 and 14 could contain the substructures of indole, carbazole, and benzocarbazole, respectively, fused with thiophene or combined with a two-ring cyclic sulfide.

N_1S_2 species were detected only in JH-1, with carbon numbers in the range of 20–36 and DBEs in the range of 8–17 (Fig. 3E). Their
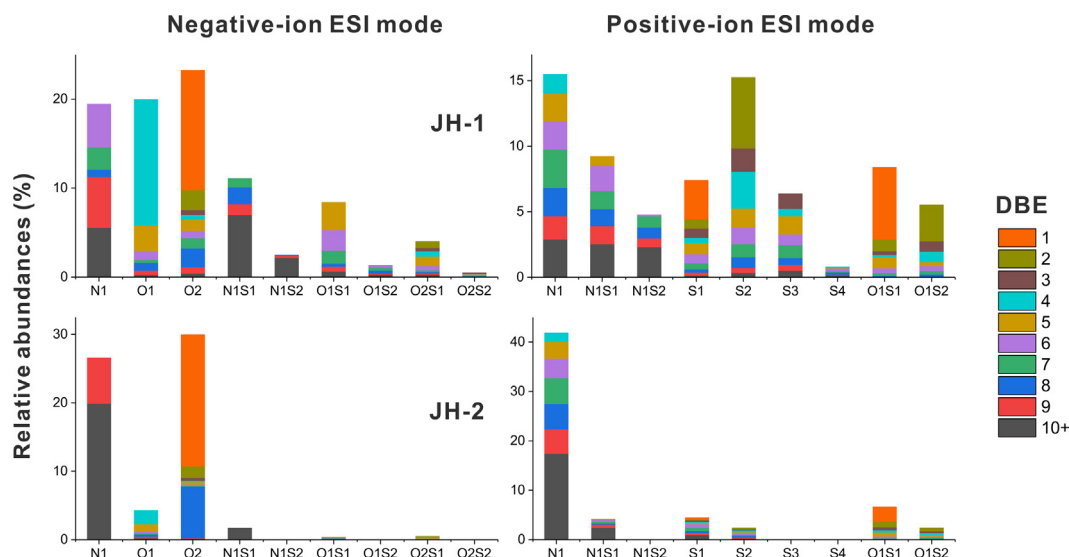

Fig. 2. Relative ion abundances of heteroatom-containing classes assigned from the ESI FT-ICR mass spectra of crude oils (contaminants such as $C_{16}H_{30}O_2$, $C_{16}H_{32}O_2$, $C_{18}H_{34}O_2$, $C_{18}H_{36}O_2$, $C_{17}H_{26}O_4$, were excluded).
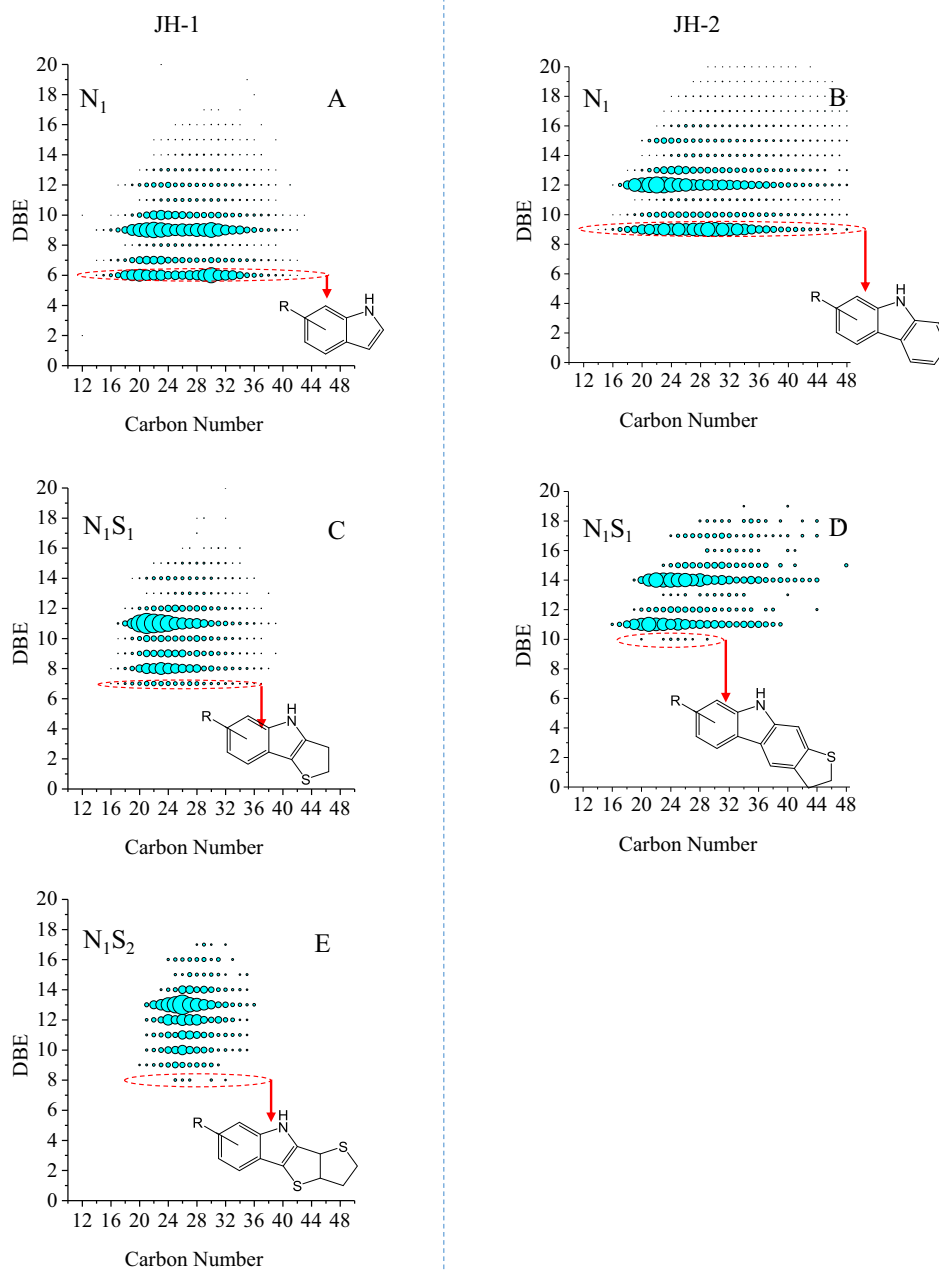
Negative-ion ESI

Fig. 3. DBE vs carbon number distributions of the N_1 and N_1S_x species in JH-1 and JH-2 analyzed by negative-ion ESI mode. The size of the circles corresponds to the relative ion abundance in the spectra. The possible structures of the species in dashed circles are also shown.

minimum DBE is higher than that of N_1 species by 2. By extrapolation from assignments of the N_1 species, N_1S_2 species with a DBE of 8 could contain an indole substructure and two saturated sulfur rings.

3.4. N_1 and N_1S_x species detected by positive-ion ESI

With NH$_4$COOH as ionization promoter, neutral nitrogen compounds and aromatic hydrocarbons can be ionized by positive-ion ESI (Lu et al., 2016). N_1 species found in the JH-1 and JH-2 oils range in carbon numbers from 12 to 50 and 14 to 48 and in DBEs from 4 to 15 and 4 to 20, respectively (Fig. 4A and B). The minimum DBE value of 4 indicates that the N_1 species under positive-ion ESI

mode are most likely basic nitrogen compounds containing pyridinic structures (Qian et al., 2001; Bae et al., 2010; Shi et al., 2010b). The N_1 species with DBEs ≥5 could contain additional naphthenic/aromatic rings with a pyridinic substructure (Shi et al., 2010b). A series of N_1 species with carbon number of 40 and DBEs of 6–9 are abundant in both oils.

N_1S_x species were detected under positive-ion ESI mode. Nitrogen heterocycles are considerably more polar than most sulfur functional groups (Liu et al., 2010a; Shi et al., 2010b; Chen et al., 2014). The distributions of detected N_1S_x species are similar whether HCOONH$_4$ was added or not, suggesting that the ionization of these N_1S_x species are mainly due to the nitrogen atom in the pyridinic substructure. In other words, the N_1S_x species can
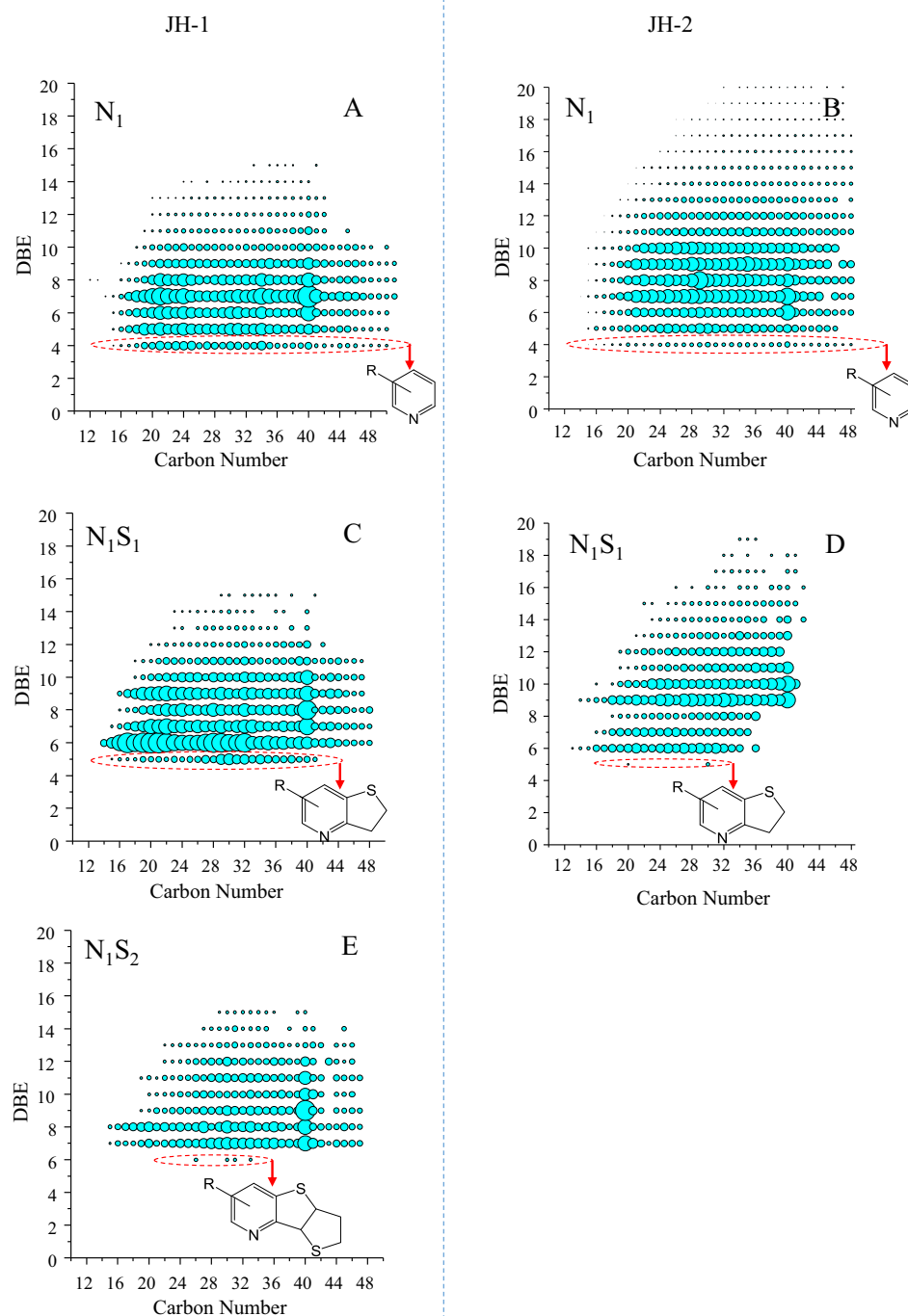
Positive-ion ESI

JH-1   JH-2

Fig. 4. DBE vs carbon number distributions of the N_1 and N_1S_x species in JH-1 and JH-2 analyzed by positive-ion ESI mode. The size of the circles corresponds to the relative ion abundance in the spectra. The possible structures of the species in dashed circles are also shown.

be considered as sulfur-containing basic nitrogen compounds. N_1S_1 species in JH-1 and JH-2 range in carbon numbers from 14 to 48 and 14 to 42, in DBEs from 5 to 15 and 5 to 19, respectively (Fig. 4C and D). The minimum DBE of N_1S_1 species in the crude oils is 5, one higher than that of the N_1 species, consistent with a pyridinic substructure with a saturated sulfur ring. N_1S_2 species are detected only in JH-1, with carbon numbers in the range 15–48 and DBEs in the range 6–15 (Fig. 4E). These compounds have a minimum DBE of 6, which is assigned to a pyridinic substructure

combined with two saturated sulfur rings. Moreover, a series of C_{40} N_1S_x compounds are also present in relatively high abundances as in the case of N_1 species, although their DBEs are different.

3.5. O_1 and O_1S_x species detected by negative-ion ESI

O_1 species detected under negative-ion ESI mode contain a hydroxyl moiety (Hughey et al., 2002b; Pan et al., 2013, 2017). O_1 species in JH-1 and JH-2 range in carbon number from 12 to
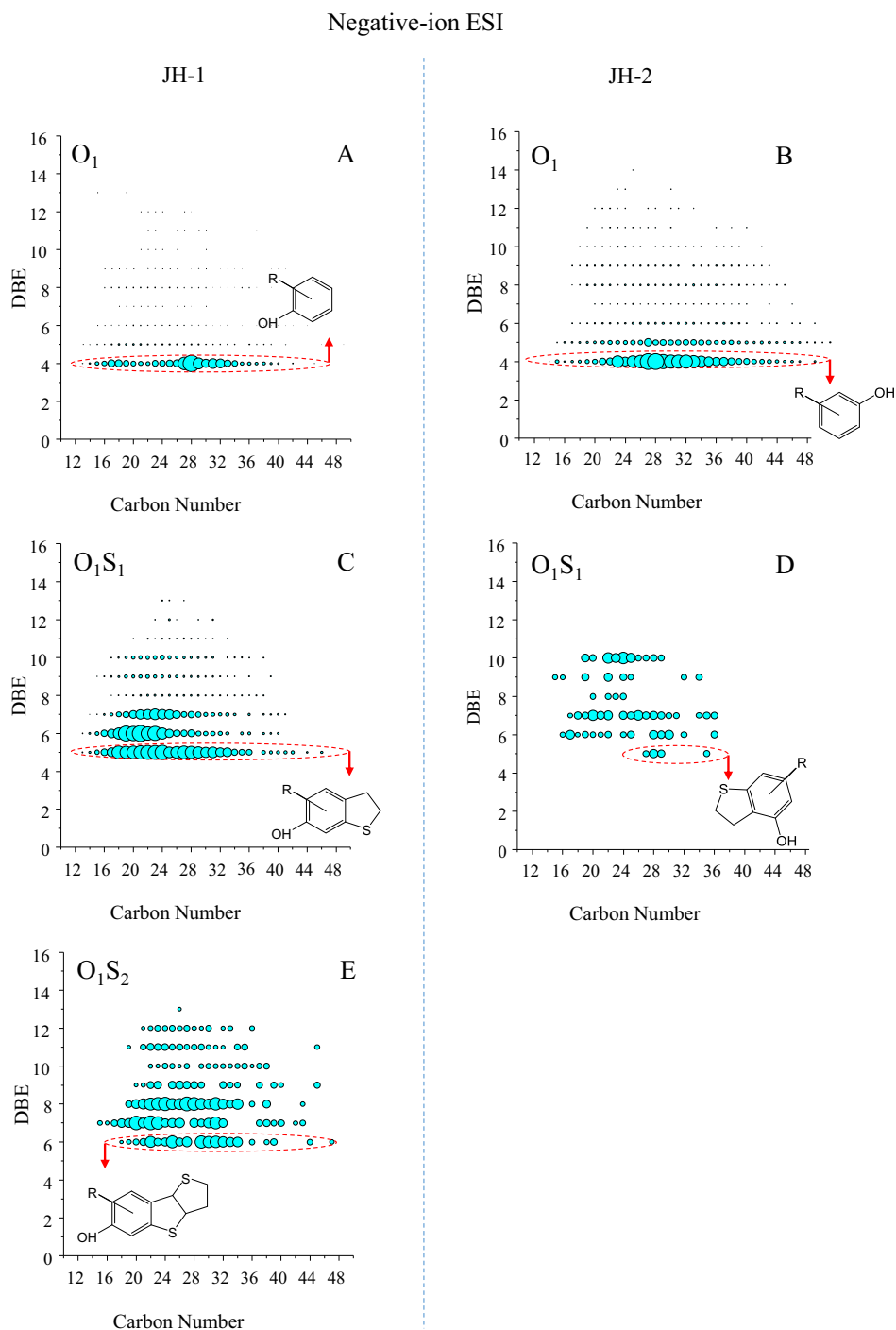
Negative-ion ESI

Fig. 5. DBE vs carbon number distributions of the O_1 and O_1S_x species in JH-1 and JH-2 analyzed by negative-ion ESI mode. The size of the circles corresponds to the relative ion abundance in the spectra. The possible structures of the species in dashed circles are also shown.

45 and 14 to 50, and in DBEs from 4 to 13 and 4 to 14, respectively (Fig. 5A and B). Compounds with a DBE of 4 are the most abundant O_1 species, which are most likely alkyl phenols (Pan et al., 2013, 2017) with the most abundant C_{28} species likely corresponding to an isoprenoid phenol (Zhang et al., 2011), although sterols are also possible (Oldenburg et al., 2017). The O_1 species with DBEs ≥5 are assigned to phenols with additional naphthenic/aromatic rings. For example, O_1 species with a DBE of 7 could be naphthols (Pan et al., 2017).

O_1S_x species detected under negative-ion ESI mode should also contain a hydroxyl moiety since sulfur functional groups generally

cannot be ionized by negative-ion ESI (Liu et al., 2010a, 2010b; Shi et al., 2010a; Lu et al., 2014). O_1S_1 species in JH-1 and JH-2 range in carbon number from 14 to 40 and 15 to 36, and in DBEs from 5 to 14 and 5 to 10, respectively (Fig. 5C and D). The minimum DBE of O_1S_1 species is 5, one higher than that of O_1 species, suggesting the presence of a phenolic substructure with a saturated sulfur ring. O_1S_2 species were detected only in JH-1, with carbon numbers in the range 16–40 and DBEs in the range 6–13 (Fig. 5E). The minimum DBE of O_1S_2 species is 6, two higher than that of O_1 species, and are assigned to a phenolic substructure with two saturated sulfur rings.
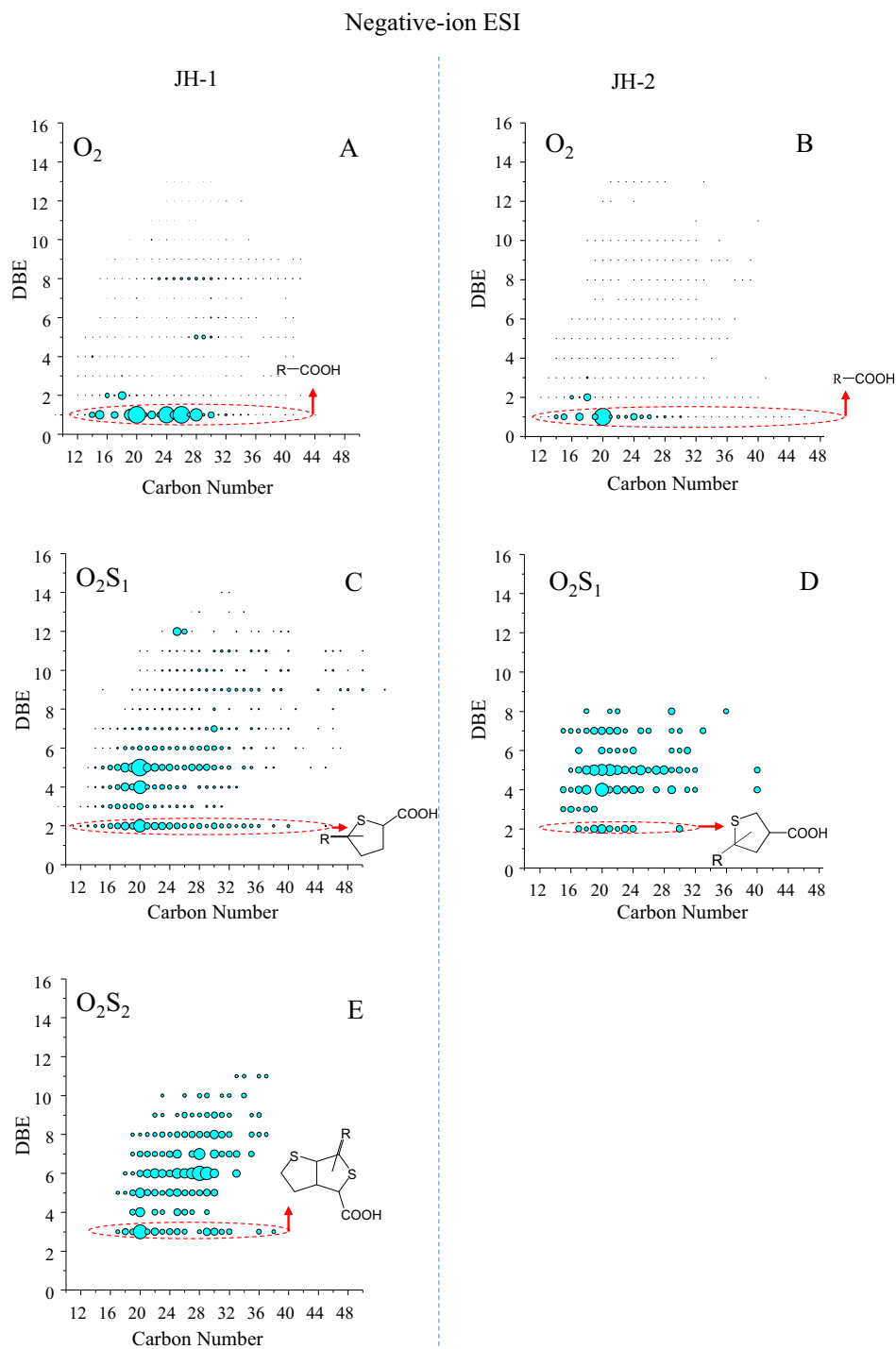
Negative-ion ESI

Fig. 6. DBE vs carbon number distributions of the O_2 and O_2S_x species in JH-1 and JH-2 analyzed by negative-ion ESI mode. The size of the circles corresponds to the relative ion abundance in the spectra. The possible structures of the species in dashed circles are also shown.

3.6. O_2 and O_2S_x species detected by negative-ion ESI

O_2 species detected under negative-ion ESI mode generally correspond to carboxylic acids (Qian et al., 2001; Hughey et al., 2002a; Liao et al., 2012; Pan et al., 2013, 2017; Shi et al., 2013; Wang et al., 2013). O_2 species in JH-1 and JH-2 range in carbon numbers from 12 to 42 and 12 to 46, respectively, possessing a similar range in DBEs from 1 to 13 (Fig. 6A and B). The compounds with a DBE of 1 are the most abundant O_2 species and likely to be fatty acids (Pan et al., 2013, 2017). These fatty acids have an even-over-odd

carbon number preference in the range C_{20}–C_{32} in both crude oils. The OEP values of fatty acids in JH-1 and JH-2 are 0.56 and 0.54, respectively. The O_2 species with DBEs ≥ 2 are assigned to naphthenic/aromatic structures containing a carboxyl moiety. For example, the O_2 species in the DBE range of 2–6 could be naphthenic acids containing 1–5 naphthenic rings (Colati et al., 2013).

O_2S_x species detected under negative-ion ESI mode are likely sulfur-containing carboxylic acids since sulfur functional groups generally cannot be ionized under negative-ion ESI mode (Liu et al., 2010a, 2010b). O_2S_1 species in JH-1 and JH-2 range in carbon
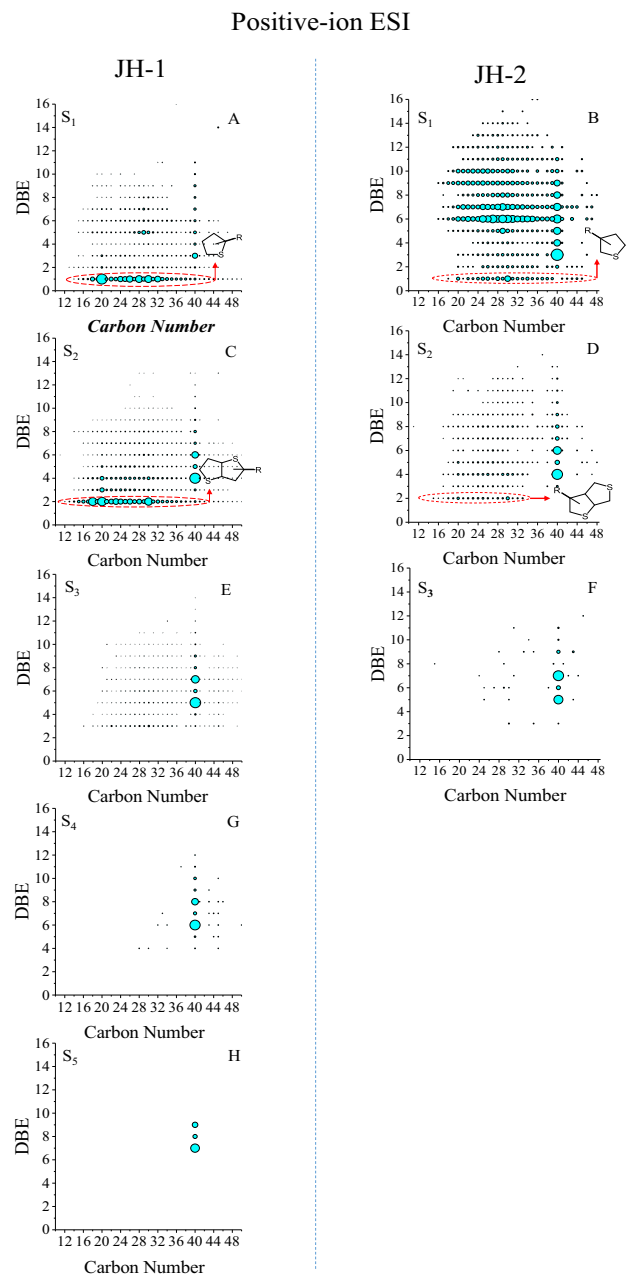
Positive-ion ESI

Fig. 7. DBE versus carbon number distributions of the S_x species in JH-1 and JH-2 analyzed by positive-ion ESI mode with the addition of HCOONH$_4$. The size of the circles corresponds to the relative ion abundance in the spectra. The possible structure of the species in dashed circles are also shown.

numbers from 12 to 40 and 15 to 32, and in DBEs from 2 to 14 and 2 to 8, respectively (Fig. 6C and D). The minimum DBE of O$_2$S$_1$ species in both crude oils is 2, which is one higher than the O$_2$ species, suggesting the presence of a carboxyl group and a saturated sulfur ring. O$_2$S$_2$ species were detected only in JH-1, with carbon numbers in the range 17–36 and DBEs in the range 3–11 (Fig. 6E). The minimum DBE of O$_2$S$_2$ species is two higher than that of O$_2$ species, suggesting a carboxyl group and two saturated sulfur rings.

3.7. S_x species detected by positive-ion ESI

Fig. 7 shows the distributions of DBE vs carbon number of S_x species by positive ESI with the addition of HCOONH$_4$ as ionization promoter (Lu et al., 2016). The maximum x value of S_x species in

JH-1 and JH-2 is 5 and 3, respectively. It is noteworthy that the minimum DBEs of S$_1$, S$_2$, S$_3$ and S$_4$ species are equal to the number of their sulfur atoms. The S$_1$ species with a DBE of 1 in the crude oils could be alkyl thiolanes or thianes. They exhibit an even-over-odd preference for carbon numbers in the range 20–32 (Fig. 7A and B), with the OEP values of 0.58 and 0.56, respectively. The S$_2$ species with a DBE of 2 are likely alkyl bi-thiolanes or bi-thianes (Fig. 7C and D). Some of these OSCs can also be detected using GC–MS (Supplementary Fig. S2). In addition, the S$_x$ species with DBE >5 may contain thiophene structures. For example, the S$_1$ species with a DBE of 6 are likely alkyl benzothiophenes. The presence of these OSCs was also reported in the immature oils of Jianghan Basin by GC–MS analysis (Fu et al., 1986; Fu and Sheng, 1989; Philp et al., 1991; Lu et al., 2014). Moreover, a series of C$_{40}$ S$_x$ species with discrete DBE distributions in the crude oils were observed.

4. Discussion

The FT-ICR MS results suggest the presence of polar OSCs with a wide range of DBEs and carbon numbers in the crude oils, together with the presence of their non-sulfur counterparts (heteroatom-containing compounds without sulfur); for example, N$_1$S$_x$ vs N$_1$ under both positive- and negative-ion ESI modes, O$_1$S$_x$ vs O$_1$ and O$_2$S$_x$ vs O$_2$ under negative-ion ESI mode. It is remarkable that the minimum DBEs of polar OSCs are slightly higher than those of their non-sulfur counterparts, with the differences equal to the number of sulfur atoms in the polar OSCs (Fig. 8). Such differences suggest the presence of sulfur rings rather than acyclic sulfur-containing groups in polar OSCs since the latter cannot contribute to the increases in DBEs (Liu et al., 2010a, 2010b).

Acyclic sulfur-containing groups are typically formed during intermolecular sulfurization (Sinninghe Damsté et al., 1988, 1989a; Tegelaar et al., 1989; Eglinton et al., 1994; Kok et al., 2000). The absence of acyclic sulfur-containing compounds in the crude oils suggests that polar OSCs in the oils are not formed through intermolecular sulfurization. On the other hand, cyclic sulfur rings, especially saturated ones, typically found in sulfurized hydrocarbons and carbohydrates are produced by intramolecular sulfurization (Sinninghe Damsté et al., 1988, 1989a). Similarly, the sulfur rings in polar OSCs also are possibly formed by intramolecular sulfurization as discussed below.

An anoxic environment with low amounts of available ferric ions (Fe^{3+}) is favorable for intramolecular sulfurization (Kohnen et al., 1990a, 1990b; Eglinton et al., 1994). The crude oils in this study were sourced from such depositional environments. The immature sulfur-rich crude oils from Jianghan Basin are generally considered to be deposited during the Eocene in a sulfate-rich hypersaline lake (Fu et al., 1986; Fu and Sheng, 1989; Philp et al., 1991; Lu et al., 2014). The water column of this hypersaline lake was periodically stratified with anoxic conditions in the photic zone (Grice et al., 1998). In this study, the crude oils show a high abundance of phytane and an even-over-odd carbon number preference of *n*-alkanes (Fig. 1), both of which are typical in anoxic depositional environments (Moldowan et al., 1985). In addition, iron mostly occurred as siderotil (FeSO$_4$·5H$_2$O) instead of Fe^{3+} ions in this area (Grice et al., 1998; Philp et al., 1991; Gao et al., 2017).

More importantly, high correlations are observed between the distributions of polar OSCs and their non-sulfur counterparts in the crude oils. Despite the presence of sulfur rings, the carbon numbers of polar OSCs are all within a similar carbon number range as their non-sulfur counterparts. Some polar OSCs even have similar or identical distribution patterns with their non-sulfur counterparts as shown on the relative ion abundance plots (Figs. 3–6). For instance, a series of C$_{40}$ compounds are relatively abundant
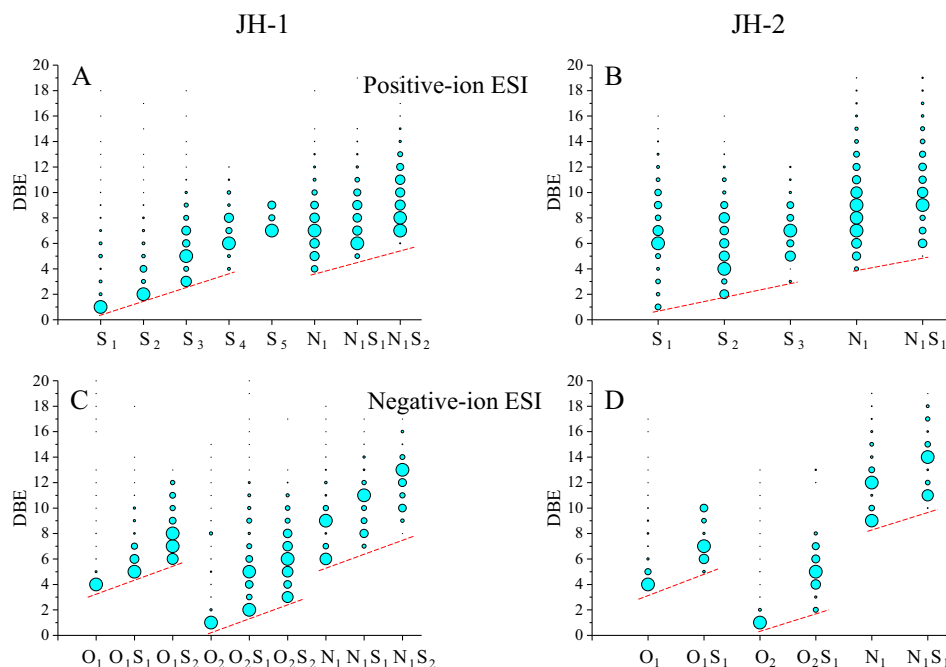
Fig. 8. The DBE distributions of the heteroatomic classes in JH-1 (A and C) and JH-2 (B and D). The size of the circles corresponds to the species' relative abundances in the corresponding class, and the size of the largest circle in each class is 1.

in the sulfur-containing basic nitrogen compounds and basic nitrogen compounds in both crude oils (Fig. 4). A similar phenomenon was observed for many sulfurized hydrocarbons/carbohydrates and non-sulfur compounds in immature oils (e.g., Sinninghe Damsté et al., 1988, 1998a; Kohnen et al., 1990). This is attributed to these compounds being derived from the same precursors but via different diagenetic reactions (e.g., Sinninghe Damsté et al., 1988, 1998a; Kohnen et al., 1990a, 1990b). For instance, Sinninghe Damsté et al. (1988) observed the presence of abundant C_{20} isoprenoid thiolane and phytane in several crude oils, which were possibly derived from phytol via intramolecular sulfurization and hydrogenation, respectively. Similarly, the high abundance of C_{40} basic nitrogen compounds and C_{40} sulfur-containing basic nitrogen compounds could also be derived from the same currently unknown precursors during early diagenesis via intramolecular sulfurization and hydrogenation, respectively. Therefore, intramolecular sulfurization should be the main formation mechanism of most of the polar OSCs in the immature oils, and the polar OSCs and their non-sulfur counterparts originate from the same precursors but via different diagenetic reactions.

Another example indicating the possible inheritance of carbon number distribution patterns is the similar even-over-odd carbon number preference shown by alkyl thiolanes/thianes (S_1 species with a DBE of 1; Fig. 7A and B), n-alkanes (Fig. 1) and fatty acids (O_2 species with a DBE of 1; Fig. 6A and B) in the oils. The fatty acids with an even-over-odd preference for carbon number in the range 20–32 are common in hypersaline environments, which may be derived from the saturated or monounsaturated fatty acids of higher plants, bacteria, and algae (Dembicki et al., 1976; Sheng et al., 1980; Elias et al., 1997). The n-alkanes with similar even-over-odd carbon number preference can be derived from fatty acids via the substitution of carboxylic group by inorganic sulfides and the subsequent breaking of the C—S bond (Sinninghe Damsté et al., 1989c; de Leeuw and Sinninghe Damsté, 1990). Therefore, we speculate that the alkyl thiolanes/thianes are, at least partially, contributed by the incorporation of inorganic sulfides into monounsaturated fatty acids via the substitution of their carboxyl group and the addition of their carbon-carbon double bond.

Intramolecular sulfurization can also reasonably explain the discrete DBE distributions of $C_{40} S_x$ compounds in the oils (Fig. 9). A possible formation mechanism of these $C_{40} S_x$ compounds could be the step-by-step intramolecular sulfurization of a carotenoid. Carotenoids are common in hypersaline environments and contain numerous conjugated carbon-carbon double bonds that are readily sulfurized or hydrogenated. (Fu and Sheng, 1989; Grice et al., 1998; Winters et al., 2013). Carotenoid-derived OSCs and alkanes have been identified in crude oils (Sinninghe Damsté et al., 1988, 1990; Sinninghe Damsté and Koopmans, 1997; Urban et al., 1999), but this is the first time that potentially carotenoid-derived OSCs with such a wide range of DBEs and sulfur atom numbers are observed. Fig. 10 displays the possible intramolecular sulfurization pathways of β-carotene. A sulfur atom can be introduced into β-carotene to form a thiolane structure via the reaction of inorganic sulfides with two conjugated double bonds. As a result, sulfurized carotenoids I–V with DBEs of 3–7 are produced through step-by-step intramolecular sulfurization. Such formation pathways provide a reasonable explanation for the occurrences of most abundant $C_{40} S_x$ species shown in Fig. 9, i.e., the S_x species ($x = 1–5$) with a DBE of $x + 2$, respectively. The thiolane structure in compounds I–V can be aromatized to more stable thiophene structure during further maturation, forming compounds VI–X with DBEs of 5–9, respectively. Such formation pathways are plausible for the second most abundant $C_{40} S_x$ species shown in Fig. 9, i.e., the S_x species ($x = 1–5$) with a DBE of $x + 4$, respectively. Moreover, all of the $C_{40} S_x$ species in JH-1 and JH-2 contain no more than five sulfur rings, which is reasonable given the symmetrical number of conjugated double bonds in β-carotene.

In addition, the number of reactive functional groups controls the feasibility of intramolecular sulfurization, evidenced by the different distribution patterns in some polar OSCs and their non-sulfur counterparts. For instance, although the C_{28} compound is abundant in the O_1 species under negative-ion ESI mode in both crude oils, the sulfur-containing $C_{28} O_1 S_x$ compounds are not as abundant (Fig. 5). This is possibly because the high abundance of $C_{28} O_1$ compound is derived from a high abundance of tocopherol
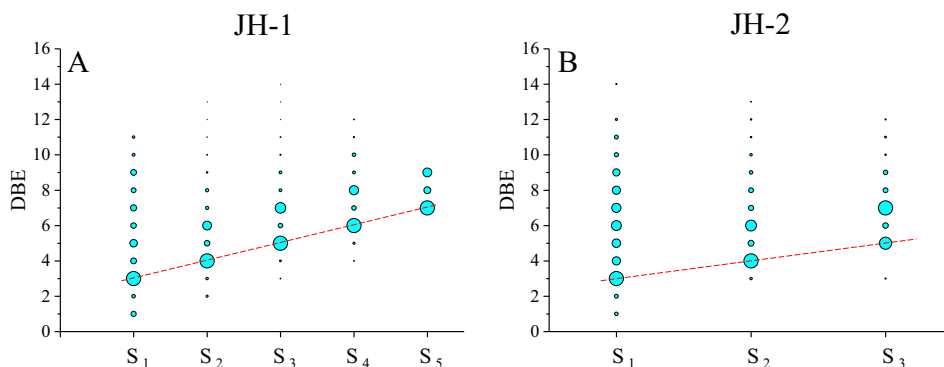
Fig. 9. The DBE distributions of the $C_{40} S_x$ species in JH-1 (A) and JH-2 (B). The size of the circles corresponds to the species' relative abundances in the corresponding class, and the size of the largest circle in each class is 1.
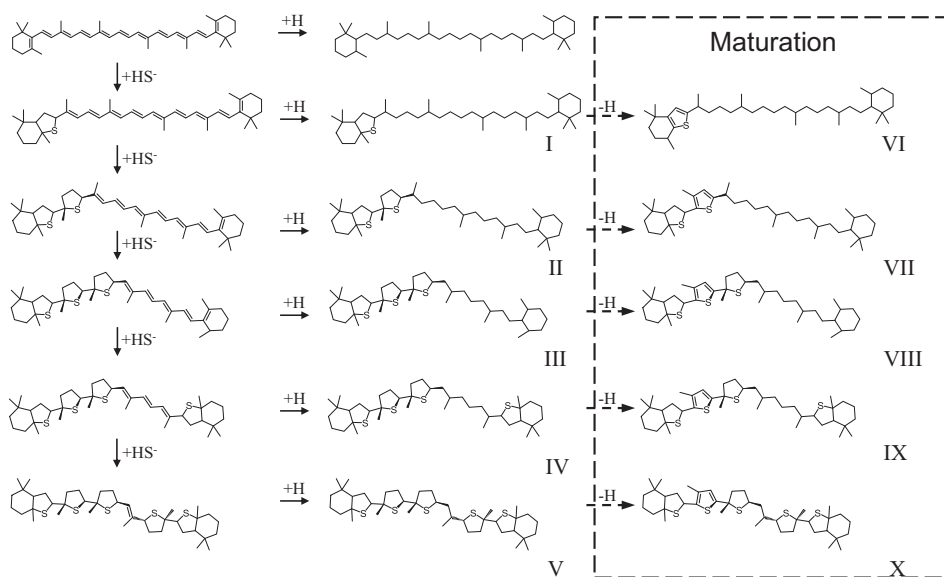

Fig. 10. Proposed formation pathways of the $C_{40} S_x$ species detected in JH-1 and JH-2. +H indicates hydrogenation process and −H indicates aromatization process. Compounds I-V are the proposed end products of intramolecular sulfurization, and they can be aromatized to compounds VI-X during maturation.

in hypersaline environments that does not contain any reactive functional groups for intramolecular sulfurization (Fu et al., 1986; Fu and Sheng, 1989; Gao et al., 2017). Therefore, the high abundance of tocopherol cannot be reflected in the polar OSCs.

The study of polar OSCs actually provides us an opportunity to hypothesize the characteristics of their precursor compounds. Polyunsaturated fatty acids are unstable and usually not very abundant in sediments (Russell et al., 2000; Niggemann and Schubert, 2006). However, through intramolecular sulfurization, their distribution patterns are likely inherited by the sulfur-containing fatty acids (Russell et al., 2000). For example, the abundant $C_{20} O_2S_1$ with a DBE of 2 and $C_{20} O_2S_2$ with a DBE of 3 (Fig. 6) could be derived from the intramolecular sulfurization of polyunsaturated fatty acids $C_{20:5}$, which are common in some planktonic algae such as diatoms (Sargent, 1976). Unlike fatty acids, the sulfur-containing fatty acids in the crude oils do not show an even-over-odd carbon number preference (Fig. 6). The OEP value of O_2S_1 species with a DBE of 2 in JH-1 is 1.00, while there are no long-chain homologues (carbon number range: 24–29) in JH-2. Therefore, it is reasonable to infer that the original polyunsaturated fatty acids did not have an even-over-odd carbon number preference either.

5. Conclusions

Our results show that the polar organic sulfur compounds (OSCs) in immature crude oils contain mainly sulfur rings in their molecular structures. These sulfur rings most likely originated from the intramolecular sulfurization of functionalized precursors during early diagenesis. The number of reactive functional groups in the precursors controls the extent of sulfurization. Precursors that do not contain reactive functional groups cannot be sulfurized, and their distribution patterns are inherited only by the non-sulfur compounds. The precursors that contain reactive functional groups such as carbon-carbon double bonds can be sulfurized intramolecularly or hydrogenated during early diagenesis, and their distribution patterns including relative abundances and even-odd carbon number preferences are inherited by the polar OSCs and their non-sulfur counterparts. For example, β-carotene having 11 conjugated double bonds can produce a series of intramolecular sulfurization products containing up to five sulfur rings. In this manner, polar OSCs could have the potential to portray the characteristics of their precursor organic matter.

Acknowledgments

Appendix A. Supplementary material

Supplementary data associated with this article can be found, in the online version, at https://doi.org/10.1016/j.orggeochem.2018. 04.003.

*Associate Editor—***Clifford Walters**

References

Andersson, J.T., 2017. Separations in the sample preparation of fossil materials for sulfur compound analysis. In: Hsu, C.S., Robinson, P.R. (Eds.), Springer Handbook of Petroleum Technology. Springer, New York, pp. 199–219.

Bae, E., Na, J., Chung, S., Kim, H., Kim, S., 2010. Identification of about 30 000 chemical components in shale oils by electrospray ionization (ESI) and atmospheric pressure photoionization (APPI) coupled with 15 T Fourier transform ion cyclotron resonance mass spectrometry (FT-ICR MS) and a comparison to conventional oil. Energy & Fuels 24, 2563–2569.

Chen, X., Liu, Y., Wang, J., Shan, H., Yang, C., Yang, C., 2014. Characterization of nitrogen compounds in coker gas oil by electrospray ionization Fourier transform ion cyclotron resonance mass spectrometry and Fourier transform infrared spectroscopy. Applied Petrochemical Research 4, 417–422.

Chen, X., Shen, B., Sun, J., Wang, C., Shan, H., Yang, C., Li, C., 2012. Characterization and comparison of nitrogen compounds in hydrotreated and untreated shale oil by electrospray ionization (ESI) Fourier transform ion cyclotron resonance mass spectrometry (FT-ICR MS). Energy & Fuels 26, 1707–1714.

Cho, Y., Ahmed, A., Islam, A., Kim, S., 2014. Developments in FT-ICR MS instrumentation, ionization techniques, and data interpretation methods for petroleomics. Mass Spectrometry Reviews 34, 248–263.

Colati, K.A., Dalmaschio, G.P., de Castro, E.V., Gomes, A.O., Vaz, B.G., Romão, W., 2013. Monitoring the liquid/liquid extraction of naphthenic acids in Brazilian crude oil using electrospray ionization FT-ICR mass spectrometry (ESI FT-ICR MS). Fuel 108, 647–655.

de Graaf, W., Sinninghe Damsté, J.S., de Leeuw, J.W., 1992. Laboratory simulation of natural sulphurization: I. Formation of monomeric and oligomeric isoprenoid polysulphides by low-temperature reactions of inorganic polysulphides with phytol and phytadienes. Geochimica et Cosmochimica Acta 56, 4321–4328.

de Leeuw, J.W., Sinninghe Damsté, J.S., 1990. Organic sulfur compounds and other biomarkers as indicators of palaeosalinity. In: Orr, W.L., White, C.M. (Eds.), Geochemistry of Sulfur in Fossil Fuels. American Chemical Society, Washington, DC, pp. 417–443.

Dembicki, H., Meinschein, W., Hattin, D.E., 1976. Possible ecological and environmental significance of the predominance of even-carbon number C_{20}–C_{30} n-alkanes. Geochimica et Cosmochimica Acta 40, 203–208.

dos Santos Rocha, Y., Pereira, R.C.L., Mendonça Filho, J.G., 2018. Negative electrospray Fourier transform ion cyclotron resonance mass spectrometry determination of the effects on the distribution of acids and nitrogen-containing compounds in the simulated thermal evolution of a Type-I source rock. Organic Geochemistry 115, 32–45.

Eglinton, T.I., Irvine, J.E., Vairavamurthy, A., Zhou, W., Manowitz, B., 1994. Formation and diagenesis of macromolecular organic sulfur in Peru margin sediments. Organic Geochemistry 22, 781–799.

Elias, V.O., Simoneit, B.R.T., Cardoso, J.N., 1997. Even n-alkane predominances on the amazon shelf and a northeast pacific hydrothermal system. Naturwissenschaften 84, 415–420.

Fu, J., Sheng, G., 1989. Biological marker composition of typical source rocks and related crude oils of terrestrial origin in the People's Republic of China: a review. Applied Geochemistry 4, 13–22.

Fu, J., Sheng, G., Peng, P., Brassell, S.C., Eglinton, G., Jiang, J., 1986. Peculiarities of salt lake sediments as potential source rocks in China. Organic Geochemistry 10, 119–126.

Gao, G., Titi, A., Yang, S., Tang, Y., Kong, Y., He, W., 2017. Geochemistry and depositional environment of fresh lacustrine source rock: a case study from the Triassic Baijiantan Formation shales in Junggar Basin, northwest China. Organic Geochemistry 113, 75–89.

Grice, K., Schouten, S., Peters, K.E., Sinninghe Damsté, J.S., 1998. Molecular isotopic characterization of hydrocarbon biomarkers in Palaeocene-Eocene evaporitic, lacustrine source rocks from the Jianghan Basin, China. Organic Geochemistry 29, 1745–1764.

Han, Y., Zhang, Y., Xu, C., Hsu, C.S., 2018. Molecular characterization of sulfur-containing compounds in petroleum. Fuel 221, 144–158.

Hsu, C.S., Liang, Z., Campana, J.E., 1994. Hydrocarbon characterization by ultra-high resolution Fourier-transform ion cyclotron resonance mass spectrometry. Analytical Chemistry 66, 850–855.

Hsu, C.S., Hendrickson, C.L., Rodgers, R.P., McKenna, A.M., Marshall, A.G., 2011. Petroleomics: advanced molecular probe for petroleum heavy ends. Special feature: perspective. Journal of Mass Spectrometry 46, 337–343.

Hughey, C.A., Rodgers, R.P., Marshall, A.G., 2002a. Resolution of 11 000 compositionally distinct components in a single electrospray ionization Fourier transform ion cyclotron resonance mass spectrum of crude oil. Analytical Chemistry 74, 4145–4149.

Hughey, C.A., Rodgers, R.P., Marshall, A.G., Qian, K., Robbins, W.K., 2002b. Identification of acidic NSO compounds in crude oils of different geochemical origins by negative ion electrospray Fourier transform ion cyclotron resonance mass spectrometry. Organic Geochemistry 33, 743–759.

Kohnen, M.E.L., Sinninghe Damsté, J.S., Baas, M., Kock-van Dalen, A.C., de Leeuw, J.W., 1993. Sulphur-bound steroid and phytane carbon skeletons in geomacromolecules: implications for the mechanism of incorporation of sulphur into organic matter. Geochimica et Cosmochimica Acta 57, 2515–2528.

Kohnen, M.E.L., Sinninghe Damsté, J.S., Kock-van Dalen, A.C., Haven, H.L.T., Rullkötter, J., de Leeuw, J.W., 1990a. Origin and diagenetic transformations of C_{25} and C_{30} highly branched isoprenoid sulphur compounds: further evidence for the formation of organically bound sulphur during early diagenesis. Geochimica et Cosmochimica Acta 54, 3053–3063.

Kohnen, M.E.L., Peakman, T.M., Sinninghe Damsté, J.S., de Leeuw, J.W., 1990b. Identification and occurrence of novel C_{36}–C_{54} 3,4-dialkylthiophenes with an unusual carbon skeleton in immature sediments. Organic Geochemistry 16, 1103–1113.

Kohnen, M.E.L., Sinninghe Damsté, J.S., ten Haven, H.L., de Leeuw, J.W., 1989. Early incorporation of polysulphides in sedimentary organic matter. Nature 341, 640–641.

Kok, M.D., Schouten, S., Sinninghe Damsté, J.S., 2000. Formation of insoluble, nonhydrolyzable, sulfur-rich macromolecules via incorporation of inorganic sulfur species into algal carbohydrates. Geochimica et Cosmochimica Acta 64, 2689–2699.

Kujawinski, E., 2002. Electrospray ionization Fourier transform ion cyclotron resonance mass spectrometry (ESI FT-ICR MS): characterization of complex environmental mixtures. Environmental Forensics 3, 207–216.

Li, M., Cheng, D., Pan, X., Dou, L., Hou, D., Shi, Q., Wen, Z., Tang, Y., Achal, S., Milovic, M., Tremblay, L., 2010. Characterization of petroleum acids using combined FT-IR, FT-ICR–MS and GC–MS: implications for the origin of high acidity oils in the Muglad Basin, Sudan. Organic Geochemistry 41, 959–965.

Liao, Y., Geng, A., Huang, H., 2009. The influence of biodegradation on resins and asphaltenes in the Liaohe Basin. Organic Geochemistry 40, 312–320.

Liao, Y., Shi, Q., Hsu, C.S., Pan, Y., Zhang, Y., 2012. Distribution of acids and nitrogen-containing compounds in biodegraded oils of the Liaohe Basin by negative-ion ESI FT-ICR MS. Organic Geochemistry 47, 51–65.

Liu, P., Shi, Q., Chung, K.H., Zhang, Y., Pan, N., Zhao, S., Xu, C., 2010a. Molecular characterization of sulfur compounds in Venezuela crude oil and its SARA fractions by electrospray ionization Fourier transform ion cyclotron resonance mass spectrometry. Energy & Fuels 24, 5089–5096.

Liu, P., Xu, C., Shi, Q., Pan, N., Zhang, Y., Zhao, S., Chung, K.H., 2010b. Characterization of sulfide compounds in petroleum: selective oxidation followed by positive-ion electrospray Fourier transform ion cyclotron resonance mass spectrometry. Analytical Chemistry 82, 6601–6606.

Lu, H., Shi, Q., Ma, Q., Shi, Y., Liu, J., Sheng, G., Peng, P., 2014. Molecular characterization of sulfur compounds in some special sulfur-rich Chinese crude oils by FT-ICR MS. Science China Earth Sciences 57, 1158–1167.

Lu, J., Zhang, Y., Shi, Q., 2016. Ionizing aromatic compounds in petroleum by electrospray with $HCOONH_4$ as ionization promoter. Analytical Chemistry 88, 3471–3475.

Moldowan, J.M., Seifert, W.K., Gallegos, E.J., 1985. Relationship between petroleum composition and depositional environment of petroleum source rocks. American Association of Petroleum Geologists Bulletin 69, 1255–1268.

Niggemann, J., Schubert, C.J., 2006. Fatty acid biogeochemistry of sediments from the Chilean coastal upwelling region: sources and diagenetic changes. Organic Geochemistry 37, 626–647.

Oldenburg, T.B.P., Jones, M., Huang, H., Bennett, B., Shafiee, N.S., Head, I., Larter, S.R., 2017. The controls on the composition of biodegraded oils in the deep subsurface – Part 4. Destruction and production of high molecular weight non-hydrocarbon species and destruction of aromatic hydrocarbons during progressive in-reservoir biodegradation. Organic Geochemistry 114, 57–80.

Pan, Y., Liao, Y., Shi, Q., 2017. Variations of acidic compounds in crude oil during simulated aerobic biodegradation: monitored by semiquantitative negative-ion ESI FT-ICR MS. Energy & Fuels 31, 1126–1135.

Pan, Y., Liao, Y., Shi, Q., Hsu, C.S., 2013. Acidic and neutral polar NSO compounds in heavily biodegraded oils characterized by negative-ion ESI FT-ICR MS. Energy & Fuels 27, 2960–2973.

Philp, R.P., Fan, P., Lewis, C.A., Zhu, H., Wang, H., 1991. Geochemical characteristics of oils from the Chaidamu, Shanganning and Jianghan basins, China. Journal of Southeast Asian Earth Sciences 5, 351–358.

Qian, K., Robbins, W.K., Hughey, C.A., Cooper, H.J., Rodgers, R.P., Marshall, A.G., 2001. Resolution and identification of elemental compositions for more than 3000 crude acids in heavy petroleum by negative-ion micro electrospray high-field Fourier transform ion cyclotron resonance mass spectrometry. Energy & Fuels 15, 1505–1511.

Russell, M., Hartgers, W.A., Grimalt, J.O., 2000. Identification and geochemical significance of sulphurized fatty acids in sedimentary organic matter from the Lorca Basin, SE Spain. Geochimica et Cosmochimica Acta 64, 3711–3723.

Sargent, J.R., 1976. The structure, metabolism and function of lipids in marine organisms. In: Malins, D.C., Sargent, J.R. (Eds.), Biochemical and Biophysical Perspectives in Marine Biology. Academic Press, London, pp. E149–E212.

Schouten, S., de Graaf, W., Sinninghe Damsté, J.S., van Driel, G.B., 1994. Laboratory simulation of natural sulphurization: II. Reaction of multi-functionalized lipids with inorganic polysulphides at low temperatures. Organic Geochemistry 22, 825–834.

Sheng, G., Fan, S., Lin, D., Su, N., Zhou, H., 1980. The geochemistry of *n*-alkanes with an even-odd predominance in the Tertiary Shahejie Formation of northern China. Physics and Chemistry of the Earth 12, 115–121.

Shi, Q., Pan, N., Liu, P., Chung, K.H., Zhao, S., Zhang, Y., Xu, C., 2010a. Characterization of sulfur compounds in oil sands bitumen by methylation followed by positive-ion electrospray ionization and Fourier transform ion cyclotron resonance mass spectrometry. Energy & Fuels 24, 3014–3019.

Shi, Q., Pan, N., Long, H., Cui, D., Guo, X., Long, Y., Chung, K.H., Zhao, S., Xu, C., Hsu, C. S., 2013. Characterization of middle-temperature gasification coal tar. Part 3: molecular composition of acidic compounds. Energy & Fuels 27, 108–117.

Shi, Q., Xu, C., Zhao, S., Chung, K.H., Zhang, Y., Gao, W., 2010b. Characterization of basic nitrogen species in coker gas oils by positive-ion electrospray ionization Fourier transform ion cyclotron resonance mass spectrometry. Energy & Fuels 24, 563–569.

Shi, Q., Yan, Y., Wu, X., Li, S., Chung, K.H., Zhao, S., Xu, C., 2010c. Identification of dihydroxy aromatic compounds in a low-temperature pyrolysis coal tar by gas chromatography-mass spectrometry (GC–MS) and Fourier transform ion cyclotron resonance mass spectrometry (FT-ICR MS). Energy & Fuels 24, 5533–5538.

Shi, Q., Zhao, S., Xu, Z., Chung, K.H., Zhang, Y., Xu, C., 2010d. Distribution of acids and neutral nitrogen compounds in a Chinese crude oil and its fractions: characterized by negative-ion electrospray ionization Fourier transform ion cyclotron resonance mass spectrometry. Energy & Fuels 24, 4005–4011.

Sinninghe Damsté, J.S., de Leeuw, J.W., 1990. Analysis, structure and geochemical significance of organically-bound sulphur in the geosphere: state of the art and future research. Organic Geochemistry 16, 1077–1101.

Sinninghe Damsté, J.S., Eglinton, T.I., de Leeuw, J.W., Schenck, P.A., 1989a. Organic sulphur in macromolecular sedimentary organic matter: I. Structure and origin of sulphur-containing moieties in kerogen, asphaltenes and coal as revealed by flash pyrolysis. Geochimica et Cosmochimica Acta 53, 873–889.

Sinninghe Damsté, J.S., Eglinton, T.I., Rijpstra, W.I.C., de Leeuw, J.W., 1990. Characterization of organically bound sulfur in high-molecular-weight, sedimentary organic matter using flash pyrolysis and Raney Ni desulfurization. In: Orr, W.L., White, C.M. (Eds.), Geochemistry of Sulfur in Fossil Fuels. American Chemical Society, Washington, DC, pp. 486–528.

Sinninghe Damsté, J.S., Irene, W., Rijpstra, C., de Leeuw, J.W., Schenck, P.A., 1988. Origin of organic sulphur compounds and sulphur-containing high molecular weight substances in sediments and immature crude oils. Organic Geochemistry 13, 593–606.

Sinninghe Damsté, J.S., Koert, E.R., Kock-van Dalen, A.C., de Leeuw, J.W., Schenck, P. A., 1989b. Characterisation of highly branched isoprenoid thiophenes occurring in sediments and immature crude oils. Organic Geochemistry 14, 555–567.

Sinninghe Damsté, J.S., Kohnen, M.E.L., Horsfield, B., 1998a. Origin of low-molecular-weight alkylthiophenes in pyrolysates of sulphur-rich kerogens as revealed by micro-scale sealed vessel pyrolysis. Organic Geochemistry 29, 1891–1903.

Sinninghe Damsté, J.S., Kok, M.D., Köster, J., Schouten, S., 1998b. Sulfurized carbohydrates: an important sedimentary sink for organic carbon? Earth and Planetary Science Letters 164, 7–13.

Sinninghe Damsté, J.S., Koopmans, M.P., 1997. The fate of carotenoids in sediments: an overview. Pure and Applied Chemistry 69, 2067–2074.

Sinninghe Damsté, J.S., Rijpstra, W.I.C., Kock-van Dalen, A.C., de Leeuw, J.W., Schenck, P.A., 1989c. Quenching of labile functionalized lipids by inorganic sulphur species: evidence for the formation of sedimentary organic sulphur compounds at the early stages of diagenesis. Geochimica et Cosmochimica Acta 53, 1343–1355.

Sinninghe Damsté, J.S., Rijpstra, W.I.C., de Leeuw, J.W., Schenck, P.A., 1989d. The occurrence and identification of series of organic sulphur compounds in oils and sediment extracts: II. Their presence in samples from hypersaline and non-hypersaline palaeoenvironments and possible application as source, palaeoenvironmental and maturity indicators. Geochimica et Cosmochimica Acta 53, 1323–1341.

Tegelaar, E.W., de Leeuw, J.W., Derenne, S., Largeau, C., 1989. A reappraisal of kerogen formation. Geochimica et Cosmochimica Acta 53, 3103–3106.

Urban, N.R., Ernst, K., Bernasconi, S., 1999. Addition of sulfur to organic matter during early diagenesis of lake sediments. Geochimica et Cosmochimica Acta 63, 837–853.

Valisolalao, J., Perakis, N., Chappe, B., Albrecht, P., 1984. A novel sulfur containing C_{35} hopanoid in sediments. Tetrahedron Letters 25, 1183–1186.

van Dongen, B.E., Schouten, S., Baas, M., Geenevasen, J.A., Sinninghe Damsté, J.S., 2003. An experimental study of the low-temperature sulfurization of carbohydrates. Organic Geochemistry 34, 1129–1144.

Wakeham, S.G., Sinninghe Damsté, J.S., Kohnen, M.E.L., de Leeuw, J.W., 1995. Organic sulfur compounds formed during early diagenesis in Black Sea sediments. Geochimica et Cosmochimica Acta 59, 521–533.

Wang, L., He, C., Zhang, Y., Zhao, S., Chung, K.H., Xu, C., Hsu, C.S., Shi, Q., 2013. Characterization of acidic compounds in heavy petroleum resid by fractionation and negative-ion electrospray ionization Fourier transform ion cyclotron resonance mass spectrometry analysis. Energy & Fuels 27, 4555–4563.

Werne, J.P., Hollander, D.J., Behrens, A., Schaeffer, P., Albrecht, P., Sinninghe Damsté, J.S., 2000. Timing of early diagenetic sulfurization of organic matter: a precursor-product relationship in Holocene sediments of the anoxic Cariaco Basin, Venezuela. Geochimica et Cosmochimica Acta 64, 1741–1751.

Werne, J.P., Lyons, T.W., Hollander, D.J., Formolo, M.J., Sinninghe Damsté, J.S., 2003. Reduced sulfur in euxinic sediments of the Cariaco Basin: sulfur isotope constraints on organic sulfur formation. Chemical Geology 195, 159–179.

Winters, Y.D., Lowenstein, T.K., Timofeeff, M.N., 2013. Identification of carotenoids in ancient salt from Death Valley, Saline Valley, and Searles Lake, California, using laser Raman spectroscopy. Astrobiology 13, 1065–1080.

Zhang, Y., Shi, Q., Li, A., Chung, K.H., Zhao, S., Xu, C., 2011. Partitioning of crude oil acidic compounds into subfractions by extrography and identification of isoprenoidyl phenols and tocopherols. Energy & Fuels 25, 5083–5089.